Advances in Adaptive Data Analysis
Vol. 2, No. 3 (2010) 295–311

DOI: 10.1142/S1793536910000495

World Scientific
www.worldscientific.com

COVERT COMMUNICATIONS BASED ON SIGNAL OVERLAY

ARNAB ROY* and JOHN F. DOHERTY†

Department of Electrical Engineering,
The Pennsylvania State University,
University Park, PA 16802-2707, USA
**aur112@psu.edu*
†*jfdoherty@psu.edu*

A covert communication technique based on the principle of signal overlay is presented here. A weak narrow-band signal is added to the primary signal and shares the same frequency band. Covertness of the overlay signal is ensured by careful signal design. At the receiver a stationary filtering approach is ineffective in separating the signals. However, the recently introduced raised cosine empirical mode decomposition technique is ideally suited to separate these time-varying signals with overlapping frequency components. An application to commercial frequency modulation overlay is presented with associated analysis and empirical performance results.

Keywords: Covert communication; signal; RCEMD.

1. Introduction

Covert communication has traditionally involved either spreading the bandwidth over which the signal is transmitted so that its power spectral density is less than that of noise or changing the carrier frequency of the signal rapidly to avoid detection. Developments in this area have given rise to the whole field of transmission security (TRANSEC) that deals with signals possessing low probability of detection (LPD), low probability of interception (LPI), low probability of exploitation (LPE) and anti-jam (AJ) features [Nicholson (1988)]. In some situations it may be useful to hide the presence or existence of the communicator's signal. Traditionally, this has meant that at an unintended receiver, the communicated signal plus receiver noise and interference cannot be reliably distinguished from just receiver noise plus interference. Therefore, LPD signals refer to those that make it difficult for unintended receivers to detect them.

Here we propose a LPD signal design strategy that aims to hide the signal under a stronger primary signal corresponding to an existing legitimate communication or broadcast service. The covert signal design ensures that it is undetectable by primary users while at the same time allows reliable recovery at the covert receiver. This concept is demonstrated here using an example of a covert transceiver on the

ground communicating with an aerial vehicle using a weak narrow-band signal. This signal is superimposed on an existing primary signal that is analogous to a cover signal. The covert receiver, at the other end, receives the composite (primary + covert) signal and extracts the weak covert signal by performing signal decomposition using the raised cosine empirical mode decomposition (RCEMD) [Roy and Doherty (2010)].

Conventional communication systems are designed such that users are separated either in the time, frequency, code or spatial domain. Traditional covert systems involve overlap in the time, frequency and spatial domains, but the users are distinguishable due to distinct codes. Here we describe a signal overlay procedure that involves signal overlap in all four domains. Successful communication between different users is possible due to distinct instantaneous frequencies (IF). We use the RCEMD algorithm to separate users based on their IFs. Distinct spatial positions and codes between the primary and covert users can be additionally used to improve the performance of the technique in terms of achievable data rate or communication range. This is achieved by the use of directional antenna by the covert transmitter to reduce the observable covert signal power by the primary receivers on the ground. Frequency hopping (FH) is also introduced to make signal detection by the unintended receiver more difficult. Further, no cooperation is assumed between the primary and covert signal transmissions and this technique does not depend upon the presence of spectral nulls in the stronger primary signal for successful communication.

Traditionally, covert signal design has involved spreading the transmission bandwidth of the secondary signal so that its power spectral density is less than that of noise to prevent unintended detection. Strategies that make this possible include the direct-sequence spread spectrum (DSSS) and ultra-wideband (UWB) signalling techniques ([Milstein *et al.* (1992)] describes a DSSS overlay system). Due to the large transmission bandwidths associated with these techniques, the primary user's signal appears as narrow-band interference (NBI) to the secondary user. For DSSS signals two classes of interference rejection techniques are used for general NBI: those based upon least-mean square estimation techniques, and those following transform domain processing principles [Milstein (1988); Iltis and Milstein (1984)]. Further, [Amin (1997); Rich *et al.* (1997); Lach *et al.* (1998); Fung *et al.* (2000)] describe DSSS overlay systems where the NBI is an angle-modulated signal, specifically a frequency modulated (FM) signal. Narrow-band interference rejection techniques in UWB systems generally follow space-time receiver strategies [Ibrahim and Buehrer (2007); Zhao and Haimovich (2002); Chang *et al.* (2006)].

Specific design considerations and performance results for this new technique are presented in the following sections. Section 2 describes this signal overlay technique in greater detail and also gives a brief overview of the RCEMD procedure that forms the basis for successful signal detection. Section 3 addresses performance issues of this communication scheme and introduces an analytical performance measure.

Simulation results are discussed in Sec. 4 while Sec. 5 presents some concluding remarks.

2. Signal Design and Decomposition Technique

The proposed overlay technique involves transmitting a weak covert signal in the same frequency band as the licensed primary signal. The covert signal is weak enough so that its presence can be ignored by the primary user. The example that we use here to illustrate the technique involves the commercial frequency modulation (FM) broadcast signal as the primary signal. For the covert signal we consider two kinds of modulation for demonstration and performance evaluation: frequency shift keying (FSK) and quadrature phase shift keying (QPSK). The covert receiver performs the RCEMD procedure on the received signal (FM + FSK/QPSK) to generate a series of elementary signal components, one of which corresponds to the transmitted FSK or QPSK signal. In the following the proposed technique is described based on the choice of FSK as the covert signal modulation. The same analysis applies to QPSK modulation also, and is therefore omitted. However in Sec. 3 where the bit-error-rate (BER) expressions for the two modulation types are different, they are presented separately. For reasonable performance on the covert signal link, the choice of frequencies used for signal insertion requires an understanding of the RCEMD technique and a brief description of the decomposition procedure follows next.

2.1. *Empirical mode decomposition*

The RCEMD technique is developed as a variation on the empirical mode decomposition (EMD) [Huang *et al.* (1998)] technique and so we first describe EMD. EMD is a method to decompose multicomponent signals that requires no *a priori* knowledge about the components. The elementary AM-FM-type signal components that are produced by the EMD procedure are called intrinsic mode functions (IMF) in literature and the extraction process is called *sifting*. The goal of sifting is to sequentially remove the higher frequency components until only the low frequency components remain. Given a signal $x(t)$ the sifting procedure divides it into a high frequency detail, $d(t)$, and the low frequency residual (or trend), $m(t)$, so that $x(t) = m(t) + d(t)$. This detail becomes the first IMF and the sifting process is repeated on the residual, $m(t) = x(t) - d(t)$. The residual signal is approximated by the mean of the maximum and minimum envelopes around the signal using cubic splines through the respective local extrema. The effective algorithm of EMD can be summarized as follows [Rilling *et al.* (2003)]:

(1) Identify all extrema of $x(t)$.
(2) Interpolate between minima (resp. maxima), ending up with some envelope $e_{\min}(t)$ (resp. $e_{\max}(t)$).
(3) Compute the mean $m(t) = (e_{\min}(t) + e_{\max}(t))/2$.

(4) Extract the detail $d(t) = x(t) - m(t)$.
(5) If $d(t)$ satisfies all conditions for being an IMF, then set $y_1(t) = d(t)$, the first IMF, else repeat above steps with $d(t)$.
(6) Evaluate the residual $x_1(t) = x(t) - y_1(t)$.
(7) Iterate on the residual $x_1(t)$.

Steps 1 to 4 may have to be repeated several times until the detail $d(t)$ satisfies the conditions for being an IMF. This process is called sifting and an upper limit is usually set on the number of sifting iterations allowed so that the process does not continue indefinitely.

The EMD technique decomposes the multicomponent signal into its components solely based upon the instantaneous frequencies present at any particular time. So, as long as the instantaneous frequencies of the signal components do not overlap in time the components can be extracted into distinct IMFs. However, in the event of overlap of instantaneous frequencies of components the signal decomposition algorithm fails in extracting the components into distinct IMFs and portions of each signal component appear in different IMFs. Since the technique proposed here involves two signals with overlapping instantaneous frequencies, extraction of the covert signal fails when the two instantaneous frequencies overlap. This leads to a loss of signal energy in that interval, that must be taken into account while deciding the transmission frequency of the covert signal. Although this decomposition procedure is empirical in nature, some recent works have tried to explore the theoretical aspects of EMD [Deléchelle *et al.* (2005); Rilling and Flandrin (2008); Stevenson *et al.* (2005)] as well as propose enhancements [Deering and Kaiser (2005); Meignen and Perrier (2007); Xuan *et al.* (2007); Kopsinis and McLaughlin (2008)].

2.2. *Raised cosine empirical mode decomposition (RCEMD)*

The RCEMD technique [Roy and Doherty (2010)] replaces the cubic spline interpolator used in EMD with the raised cosine pulse. The time-and frequency-domain representations of the raised cosine pulse are given by

$$h(t) = \sin c\left(\frac{\pi t}{T}\right)\frac{\cos\left(\frac{\pi\beta t}{T}\right)}{1-\frac{4\beta^2 t^2}{T^2}}, \tag{1}$$

$$H(f) = \begin{cases} T; & |f| \le \dfrac{1-\beta}{2T} \\ \dfrac{T}{2}\left[1+\cos\left(\dfrac{\pi T}{\beta}\left(|f|-\dfrac{1-\beta}{2T}\right)\right)\right]; & \dfrac{1-\beta}{2T} < |f| \le \dfrac{1+\beta}{2T}. \\ 0; & \text{otherwise} \end{cases} \tag{2}$$

respectively. The roll-off factor, β, is a measure of the *excess bandwidth* of the filter, i.e. the bandwidth occupied beyond the Nyquist bandwidth of $f_s/2$. Its value varies

between 0 and 1. Although the raised cosine filter is a viable interpolation technique when samples are uniformly spaced or follow a pattern, this condition is violated for time-varying frequencies. However, over small intervals the signal IFs may be assumed to constant, thereby allowing application of raised cosine interpolation over the interval. This is the basis of the windowed RCEMD algorithm that is used in our application. In this case the window length is five consecutive maxima or minima and the the fundamental period, T is estimated from the actual signal segments in real-time. This procedure automatically adapts the filter coefficients according to the present IFs within the data segment. In our simulations the window length corresponds to five consecutive peaks as it was found to be the best compromise between complexity and performance.

The choice of RCEMD here is based on its superior signal separation properties [Roy and Doherty (2010)] compared to the original EMD procedure. Results comparing the performance of the RCEMD to EMD are presented in Fig. 3 and Fig. 4. In Fig. 3 decomposition quality of RCEMD technique for various frequency and amplitude ratios of two tones is presented in a format similar to that of Fig. 3 in [Rilling and Flandrin (2008)]. In the figure a performance measure of the separation quality for two tones is presented after 100 iterations of the RCEMD algorithm. From the figure it is clear that the transition region between good and bad separation regions (denoted by light and dark shades in the figure respectively) lies to the right of the line representing the equation $\frac{A_2}{A_1}\left(\frac{f_2}{f_1}\right)^2 = 1$, whereas the corresponding region for EMD lies to the left of the line (as seen from Fig. 3 in [Rilling and Flandrin (2008)]), signifying better signal separation quality for RCEMD. Finally, performance of the two algorithms in identifying the frequency components present in $\cos^3(2\pi ft)$ is shown in Fig. 4. The signal components at frequencies f and $3f$ are correctly identified by the RCEMD algorithm, whereas the EMD algorithm fails to do so.

2.3. *Signal design*

Formally, the received signal at the legitimate receiver as well as the covert receiver may be represented as

$$r'(t) = r'_p(t) + r'_s(t) + n'(t) \tag{3}$$

where $r'_p(t)$ and $r'_s(t)$ represent the legitimate primary and added covert (or secondary) signals respectively and $n'(t)$ is the additive white Gaussian noise (AWGN). The covert transmitter and receiver are located within the FM broadcast region. The maximum separation between the two is determined by the maximum overlay signal strength that can be transmitted without causing noticeable interference to nearby FM receivers and by the maximum allowable BER at the covert receiver. A more thorough discussion on these constraints is presented in the following sections. At the covert receiver, the combined FM broadcast plus FSK signal having a bandwidth of $B\ Hz$ is first frequency shifted to a range of

$0 - B\ Hz$, generating a complex-valued signal. The RCEMD procedure is then applied to the down-converted signal to extract the covert signal. Figure 1 shows the block diagram of the covert receiver. In this case, f_{FM} is the center frequency of the commercial FM band and the intermediate frequency, $f_I = B/2\ Hz$. After down-conversion the complex-valued signals are denoted in the same fashion as in (3), but without the primes. Frequency spectrums of the primary and covert signals are shown in Fig. 2. The validity of the technique is demonstrated by applying complex-valued RCEMD algorithm to the combined signals in the following sections.

The reason for the frequency down-conversion step follows. As pointed out in [Roy and Doherty (2008); Rilling and Flandrin (2008)] in the context of separation of pure tones of frequencies f_1 and f_2 ($f_1 > f_2$), the quality of extraction

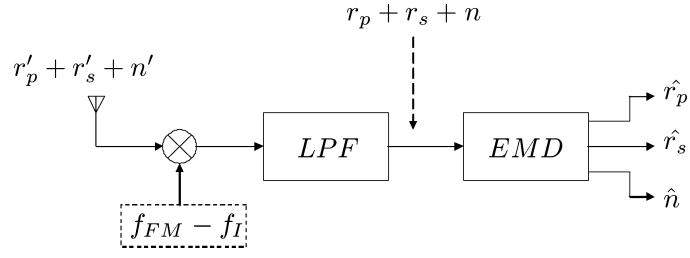

Fig. 1. Block diagram of the covert receiver.

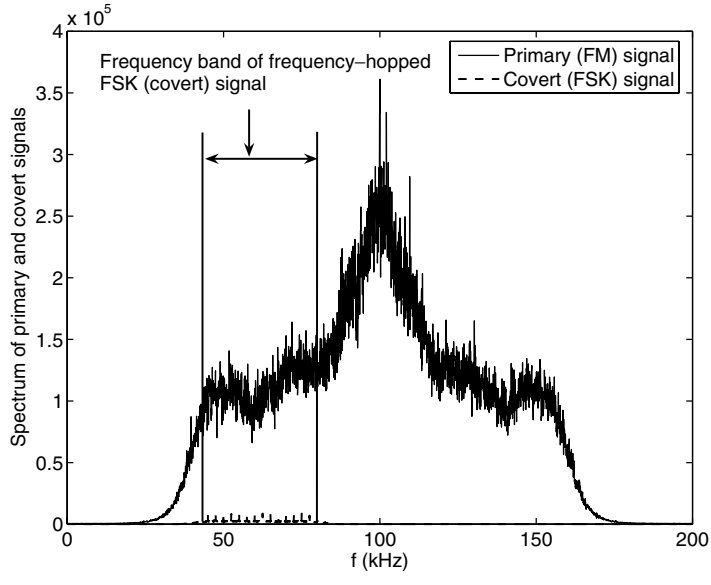

Fig. 2. Frequency domain representation of the primary (FM) and frequency-hopped covert (FSK) signals shown here. The primary signal power is 26 dB larger than that of the FSK signal in this illustration.

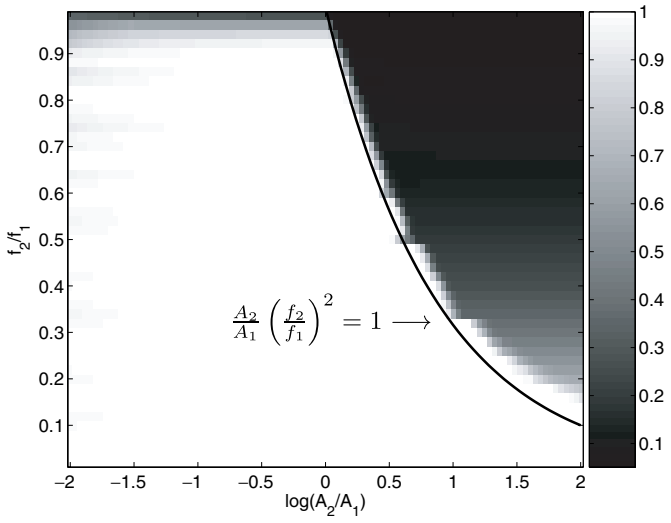

Fig. 3. Final value of the performance metric measuring decomposition quality for pure tones after 100 iterations of the RCEMD algorithm is plotted for a range of amplitude and frequency ratios. A curve representing the theoretical limit for successful signal separation by EMD [Rilling and Flandrin (2008)] is also drawn.

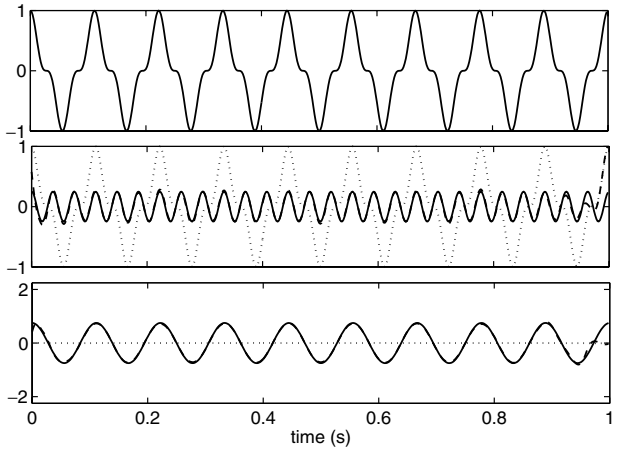

Fig. 4. Signal decomposition quality comparison between RCEMD and EMD algorithms for $\cos^3(2\pi ft)$ is shown here. First panel shows the original signal. The other two panels show the signal components at frequencies $3f$ and f, along with the decomposition results from RCEMD (dashed) and EMD (dotted). The RCEMD lines are covered by the solid lines of the actual signal components in the lower two panels due to perfect decomposition.

depends on the ratio f_1/f_2. A larger frequency ratio for a given amplitude ratio results in better signal decomposition performance. By down-converting the signals, we increase the ratio of the IFs of the two signals even though their absolute difference remains the same resulting in better decomposition quality.

3. Performance Analysis

We demonstrate typical extraction results of the RCEMD algorithm and IFs of the FM and FSK signals in Figs. 5 and 6 respectively. Here we consider only the real part of the complex baseband signal. In general, the initial IMFs that RCEMD

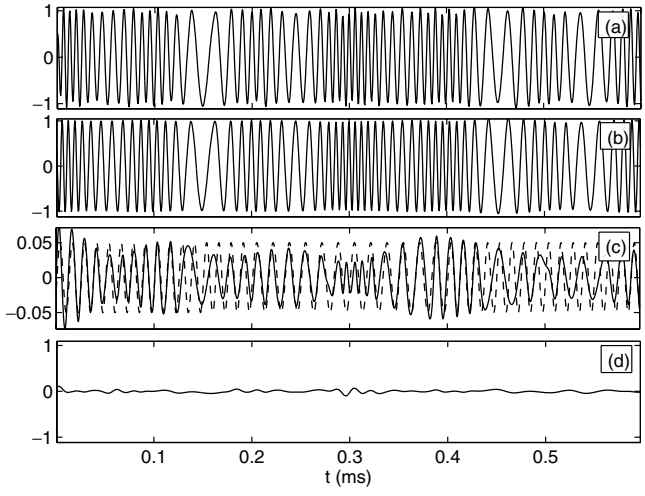

Fig. 5. Time domain representation of the composite signal (FM + FSK) and the extracted components by the EMD algorithm for a time interval extending over 5 FSK symbol durations. In (c) the actual FSK signal is shown by the dashed curve. Only real parts of the complex signals are shown.

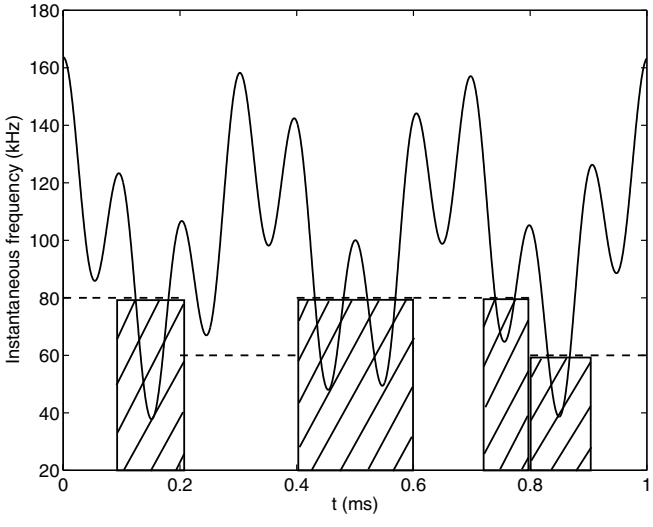

Fig. 6. Instantaneous frequencies of the FM signal (solid) and the FSK signal (dashed) for a time interval extending over 5 FSK symbol durations. The hatched area indicates the times when signal decomposition is not possible. Frequency hopping of the covert signal is turned off for clarity.

generates contain the high frequency components of the signal, including noise, and the subsequent IMFs contain the lower frequency components [Kopsinis and McLaughlin (2008)]. Figure 5(a) shows the composite signal (FM + FSK) as received at the secondary receiver for a low noise case and the extracted components are shown in Figs. 5(b)–5(d). Clearly, the first component corresponds to the FM signal, the second resembles the overlaid FSK signal and the remaining components (of which only the third is shown in the figure) contain the residual FSK signal energy. Upon close observation of the FSK waveform and the second IMF in Fig. 5(c), it is evident that although the second component closely approximates the original signal over certain intervals, at other times it deviates from the original due to superimposed amplitude and frequency modulations.

The superimposed amplitude modulated (AM) signal and the newly introduced frequencies in the second component can be explained based on the IFs of the two signals, shown in Fig. 6. For an FM signal represented by

$$r_p(t) = A_p \cos\left[2\pi f_I t + k_f \int_{-\infty}^{t} m(\tau)d\tau\right] \tag{4}$$

the IF is given by [Lathi (1998)]

$$f_{\text{inst}} = f_I + \frac{k_f}{2\pi} m(t) \tag{5}$$

where k_f represents the frequency-deviation constant, $m(t)$ is the modulating signal and A_p is the amplitude of the FM signal. This IF is shown in Fig. 6 for an arbitrary modulating signal. The IF of the FSK signal is also shown in the figure. Due to the intersecting IFs, common nonstationary signal decomposition techniques result in poor signal decomposition quality. However, using the RCEMD procedure, when the IF of the primary signal is significantly larger than that of the secondary signal, extraction is successful and high fidelity separation of the signal components occurs. When the primary signal's IF is either close to that of the secondary signal or smaller, the extraction fails to produce a component that contains a useful copy of the FSK signal. The algorithm fills the interval with a signal having smoothly varying amplitude and random frequency to maintain phase continuity with the correctly extracted portion of the secondary signal. The affected intervals are shown by the hatched area in Fig. 6. To avoid this phenomenon, the overlay FSK frequencies are chosen such that they are smaller than the IF of the primary signal with high probability. Thus, frequencies near the lower edge of frequency band of the primary signal are selected for transmitting the secondary signal. Moreover, the EMD and the RCEMD algorithms are more effective in signal separation when the stronger signal has a larger IF [Roy and Doherty (2008)].

In the proposed technique signal decomposition is terminated at the first level, i.e., only two signal components are generated. The reasoning behind this choice is that the signal decomposition technique always produces a close approximation of the FM signal as the first component and the FSK signal energy is split among the remaining components. Therefore, terminating the decomposition procedure after

the second component is generated prevents the splitting of the FSK signal energy into multiple components and this improves signal estimation reliability.

3.1. *Error rate performance*

Here we develop a model for the extracted secondary signal using RCEMD that leads to a simple formula to calculate the BER. Based on the above discussion, it is clear that second component generated by the algorithm is a high fidelity approximation of the original FSK signal over the interval when the IF of the FM signal exceeds that of the FSK signal, and has little resemblance to the transmitted signal when the order of the IFs gets reversed. So corresponding to the two conditions we model the second component either as an exact copy of the transmitted FSK signal or as a signal with random frequency and amplitude over the respective intervals. As a result, the cross-correlation coefficient between the segments of the second component containing random frequencies and the original FSK signal is zero, on average. To model this, we represent by T_1 and T_2 the average amount of time within an FSK bit interval, T, that the two FSK frequencies are larger than the FM IF, f_{inst}. The secondary BER can then be derived by suitably adjusting the E_b/N_0 value in the standard non-coherent FSK result to reflect the fraction of the total signal energy that is useful in FSK detection. Then the resulting BER for non-coherent FSK is

$$P_b = \frac{1}{2} e^{-\frac{1}{2}\left(\frac{E_b}{N_0}\right)_{\text{eff}}} \tag{6}$$

where

$$\left(\frac{E_b}{N_0}\right)_{\text{eff}} = \frac{E_b}{N_0}(1-\xi) \tag{7}$$

and $\xi = \frac{T_1+T_2}{T}$ is the time fraction for which the FSK IF is larger than f_{inst}. As a result, $(1-\xi)$ represents the fraction of the signal energy that contributes to successful symbol detection. An analogous expression for BER when the covert signal is QPSK modulated is

$$P_b = \frac{1}{2} erfc\left(\sqrt{\left(\frac{E_b}{N_0}\right)_{\text{eff}}}\right) \tag{8}$$

where $\xi = \frac{T_1}{T}$ is substituted in (7) for the time fraction for which the QPSK signal frequency is larger than the FM IF, f_{inst}. Given the covert signal transmission frequencies, the time fraction (ξ) can be easily derived mathematically. The BER calculated using this simple model is shown along with simulation results in Sec. 4 (Fig. 9), where close agreement is observed.

4. Simulation Results

To improve the degree of covertness of the inserted signal we employ the FH principle. In this example we use slow FH with 16 hop frequencies to reduce signal

detection probability by an unintended receiver. The BER-vs-E_b/N_0 results when the covert signal is FSK and QPSK modulated are shown in Figs. 7 and 8 respectively. For these results, the received covert signal was 26 dB weaker than the FM signal. Hop frequencies were confined within a band stretching from 0.4 B to 0.8 B. Also, secondary data transmission rate of 5 kbps was simulated and an

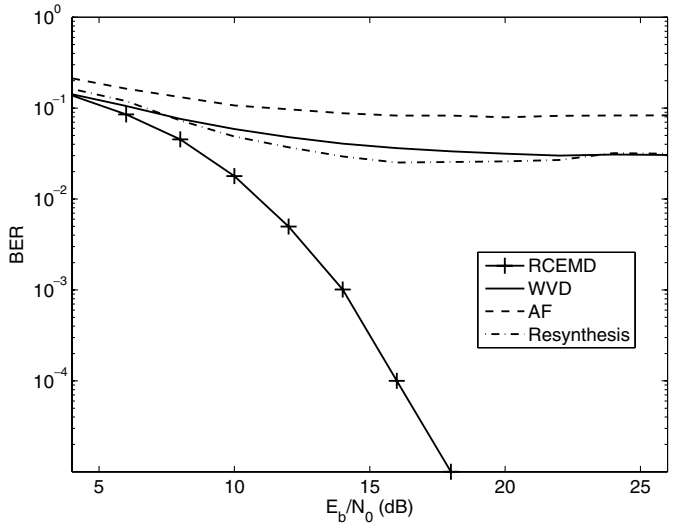

Fig. 7. E_b/N_0-vs-BER plots when covert transmitter uses FSK modulation. Frequency hopping is used with 16 hop frequencies.

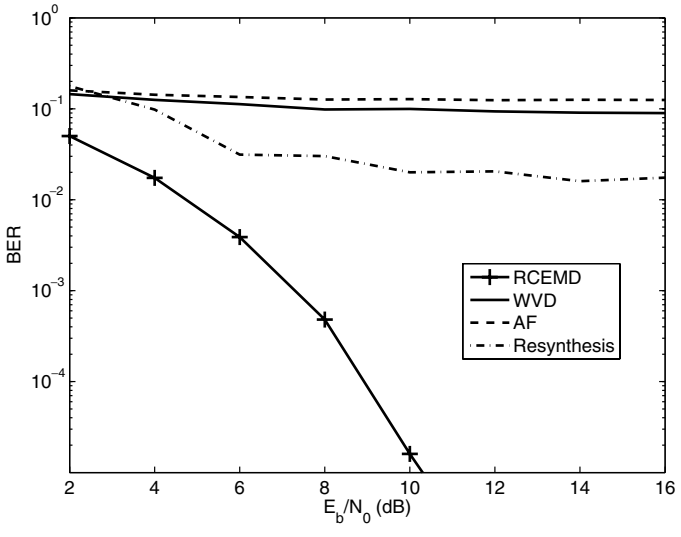

Fig. 8. E_b/N_0-vs-BER plots when covert transmitter uses QPSK modulation. Frequency hopping is used with 16 hop frequencies.

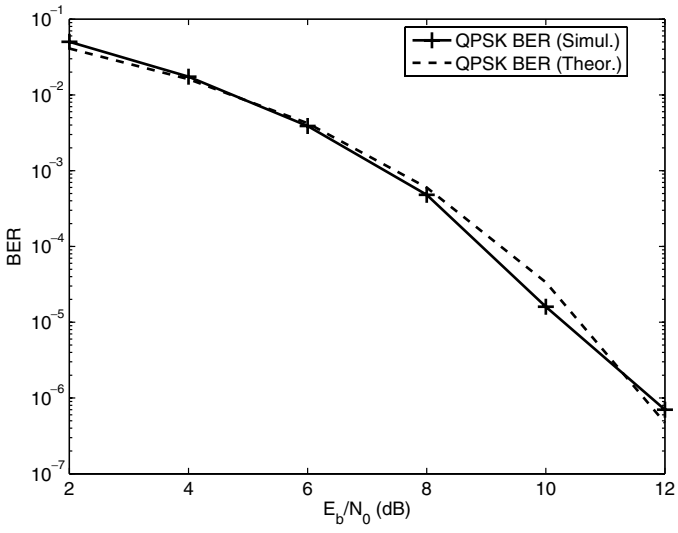

Fig. 9. Comparison of the BER values obtained using the simple model developed in text (Equation 8) and simulation results for QPSK modulated covert signal. Ratio of primary to covert signal power is 26 dB here.

over-sampling factor of 10 was employed. So, voice communications and low-rate data communications using error-correcting codes are possible applications of this overlay scheme. For our experiments the FM modulating signal is modeled as a filtered noise output of a first-order auto-regressive (AR(1)) model.

In Figs. 7 and 8 BER performance results for three alternate techniques are also presented. The first method is a two-step procedure where the IF of the FM signal is first estimated using the Wigner-Ville distribution (WVD) and then a short, time-varying finite impulse response (FIR) notch filter is designed to remove that frequency [Amin (1997)]. The time-varying nature of the primary signal requires a short length notch filter, which corresponds to a wide notch in the frequency domain, thereby significantly distorting the secondary signal. In the original scenario in [Amin (1997)] since the interference (FM) signal occupied a small fraction of the frequency band of the signal of interest (DSSS signal), distortion of the entire band of frequencies containing the interferer was negligible. However, in the present case a wide notch filter, in addition to eliminating the primary signal, also severely degrades the secondary signal. Secondly, we study the performance of a simple adaptive filter (AF) based on the least-mean-square (LMS) algorithm at removing the primary signal at the secondary receiver. Poor signal separation quality results due to similarity of the autocorrelation functions of the constituent signals and due to the time-varying nature of the primary signal.

The final method that we study involves subtracting a resynthesized FM signal from the received signal to generate the FSK signal. We use a first-order phase locked loop (PLL) to demodulate the FM signal from the received composite signal

(FM+FSK). The estimated modulating signal, thus derived, is then used to remodulate a carrier signal which when subtracted from the received signal produces an estimate of the secondary FSK signal. However, due to the noisy input to the PLL, the resynthesized FM signal is not identical to the original FM signal, resulting in the appearance of some FM signal energy in the difference. It is observed from results that the BER for this resynthesis technique saturates for large E_b/N_0 because the residual phase error at PLL output due to noisy input (FM+FSK+thermal noise) is essentially limited by the FSK signal amplitude, which is independent of E_b/N_0. When QPSK is used for modulating the covert signal the BER saturates at large E_b/N_0 due to the same reason as seen in Fig. 8.

Finally, we demonstrate the relative decomposition quality of the different techniques introduced above. Figure 10 presents the estimate of the covert signal obtained using the four methods considered in the paper, superimposed on the original covert signal. Although severe distortion due to the AF technique is evident, the RCEMD, WVD and Resynthesis results appear better, with the RCEMD output resembling the original signal the most. A quantitative measure of the decomposition quality is shown in Fig. 11, where the normalized mean-squared-error (NMSE) between the extracted components using different techniques and the original signal is presented for varying E_b/N_0.

4.1. *Communication range determination*

The maximum communication range for the covert users is limited by two constraints. The minimum SNR required at the covert receiver for reliable signal detection is one constraint. Large transmit power is desirable in this case. The other requirement is that users of the primary signal in the vicinity of the covert transmitter be unaffected by the inserted signal. This requires small transmit power. It is

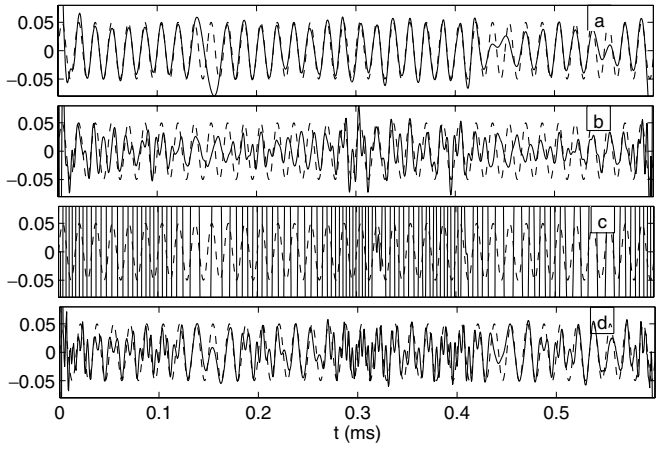

Fig. 10. Estimate of the covert signal obtained using the four techniques: (a) RCEMD, (b) WVD, (c) AF and (d) Resynthesis superimposed on the original covert signal.

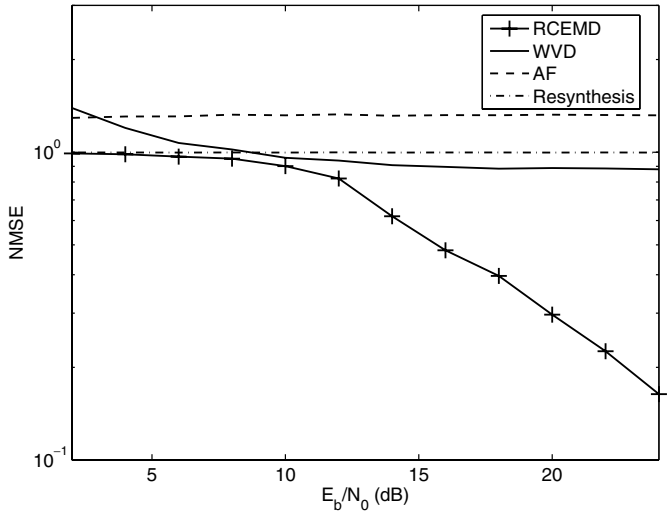

Fig. 11. NMSE between the actual and extracted covert signal using the four algorithms described in text.

evident that the two requirements place opposing constraints on the transmit signal power. To calculate the useful communication range for this technique we first find the largest allowable transmit power for the covert user that allows normal signal reception by nearby primary users and then find the maximum range at which the covert receiver can be located for reliable signal detection for this power level.

To analyze the effect of the secondary (covert) signal on the users of the primary signal we note that at any instant the FSK signal appears as a tone interferer to the FM receiver. It has been shown that the output of an ideal frequency demodulator due to a tone interferer is given by [Lathi (1998)]

$$y_s(t) = \frac{A_s}{A_p} 2\pi(f_I - f_k)\cos(2\pi(f_I - f_k)t) \tag{9}$$

where $k = 1, 2$ corresponding to the two FSK frequencies and A_p and A_s are the amplitudes of the primary and secondary (covert) signals respectively, with $A_s \ll A_p$. Since the interference output is inversely proportional to the primary signal amplitude, the weak interference is suppressed and so the interference level must be at least 6 dB weaker than the FM signal to avoid objectionable interference to the FM listener [Lathi (1998)]. A directional antenna pointed towards the aerial vehicle reduces the interference to FM receivers on the ground. Sidelobe power of −18 dB is assumed in our studies. So although this limits the secondary transmit power to 12 dB larger than the FM level, we assume that the covert transmitter transmits at only 6 dB above the primary signal level for safety. Based on these values, the maximum distance of an aerial vehicle flying at an altitude of 33,000 ft. (10,000 m) to attain a BER of 10^{-5} (corresponding to E_b/N_0 of approximately 18 dB and 11 dB from Figs. 7 and 8 for FSK and QPSK modulations respectively)

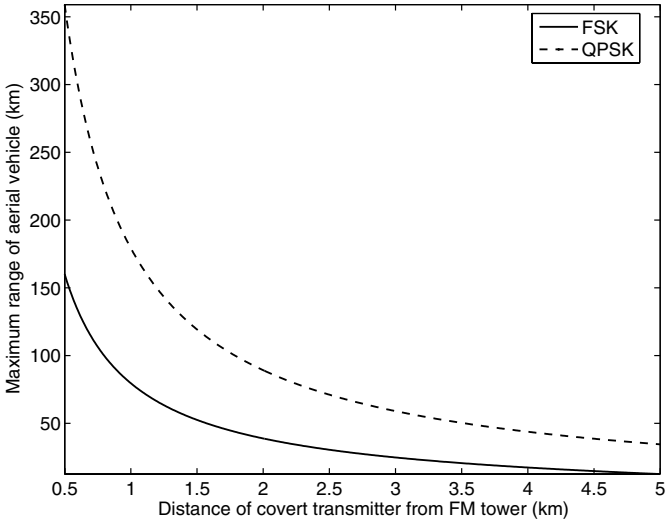

Fig. 12. Maximum horizontal range of the aerial vehicle flying at an altitude of 33,000 ft. (10,000 m) to achieve BER of 10^{-5} as a function of separation between the FM and covert transmitters. Maximum ranges for the two modulation types considered in the text are shown.

is presented in Fig. 12 for various distances of the covert transmitter from the FM tower. The reason for the drop in range of the covert communication as the transmitter is placed farther away from the FM tower follows from our discussion above where it was pointed out that the power of the covert transmitter depends upon the FM signal power at the location. Due to decrease in primary signal power away from the FM tower, the covert transmitter is required to reduce its transmit power to prevent interference to neighboring primary users. This reduces its effective communication range. However, in the reverse direction (from aerial vehicle to ground) the power constraint is less stringent as the covert signal is required to be weaker than the primary signal only near ground level and so the aerial vehicle can transmit at a higher power level than the transmitter on ground. Therefore, the effective range of this system is decided by power requirements in the ground-to-air direction.

5. Conclusions

A technique for covert communications between a transceiver located on the ground and another on an aerial vehicle using signal overlay has been demonstrated here. By transmitting a weak signal in a frequency band occupied by another stronger signal reliable communication is possible by performing signal decomposition using the RCEMD algorithm. The RCEMD procedure separates the two signals at the covert receiver based on their instantaneous frequencies. Probability of detection by an unintended receiver is minimized due to masking by the strong primary signal. Frequency hopping further reduces the probability of detection by the unintended

receiver. Moreover, the use of directional antenna by the covert transmitter to communicate with the receiver located on an aerial vehicle reduces the interference caused to nearby FM receivers.

This technique makes possible covert voice communication and data transmission from unattended sensors in possibly hostile territories. Resistance to jamming is guaranteed for this technique due to the difficulty of the jammer to jam the covert signal without significantly distorting the primary signal. Performance of this technique in terms of achievable BER and communication ranges was studied.

References

Amin, M. G. (1997). Interference mitigation techniques in spread spectrum communication systems using time-frequency distributions. **45**: 90–101.

Chang, T.-H., Chi, C.-Y. and Chang, Y.-J. (2006). Space-time selective RAKE receiver with finger selection strategies for UWB overlay communications. **54**: 1731–1744.

Deering, R. and Kaiser, J. F. (2005). The use of a masking signal to improve empirical mode decomposition, in *Proc. IEEE Int. Conf. Acoust., Speech Signal Process.* (*ICASSP*), Philadelphia, PA.

Deléchelle, E., Lemoine, J. and Niang, O. (2005). Empirical mode decomposition: An analytical approach for sifting process. *IEEE Signal Process. Lett.*, **12**: 764–767.

Fung, H. W., Kot, A. C. and Li, K. H. (2000). A novel approach to FM interference suppression in DS spread-spectrum communication systems, in *Proc. 2000 IEEE Int. Conf. Acoust., Speech and Signal Process.*, Istanbul, Turkey.

Huang, N. E., Shen, Z., Long, S. R., Wu, M. C., Shih, H. H., Zheng, Q., Yen, N.-C., Tung, C. C. and Liu, H. H. (1998). The empirical mode decomposition and the Hilbert spectrum for nonlinear and non-stationary time series analysis. *Proc. R. Soc. Lond. A*, **454**: 903–995.

Ibrahim, J. and Buehrer, R. M. (2007). NBI mitigation for UWB systems using multiple antenna selection diversity. **56**: 2363–2374.

Iltis, R. A. and Milstein, L. B. (1984). Performance analysis of narrow-band interference rejection techniques in DS spread-spectrum systems. **32**: 1169–1177.

Kopsinis, Y. and McLaughlin, S. (2008). Investigation and performance enhancement of the empirical mode decomposition method based on a heuristic search optimization approach. **56**: 1–13.

Kopsinis, Y. and McLauglin, S. (2008). Empirical mode decomposition based denoising techniques, in *Proc. 2008 IAPR Workshop on Cognitive Information Processing — CIP, 2008*, Santorini, Greece.

Lach, S. R., Amin, M. G. and Lindsey, A. R. (1998). Broadband nonstationary interference excision for spread spectrum communications using time-frequency synthesis, in *Proc. 1998 IEEE Int. Conf. Acoust., Speech and Signal Process.*, Seattle, WA.

Lathi, B. P. (1998). *Modern Digital and Analog Communication Systems*, 3rd ed., Oxford University Press, New York, NY.

Meignen, S. and Perrier, V. (2007). A new formulation for empirical mode decomposition based on constrained optimization. *Signal Process. Lett., IEEE*, **14**: 932–935.

Milstein, L. B. (1988). Interference rejection techniques in spread spectrum communications. *Proc. IEEE*, **76**: 657–671.

Milstein, L. B., Schilling, D. L., Pickholtz, R. L., Erceg, V., Kullback, M., Kanterakis, G., Fishman, D. S., Biederman, W. H. and Salerno, D. C. (1992). On the fesibility of a CDMA overlay for personal communications networks. **10**: 655–668.

Nicholson, D. L. (1988). *Spread Spectrum Signal Design.* Computer Science Press, Rockville, MD.

Rich, D. A., Kermalli, M. H., Cassara, F. A. and Benson, J. J. (1997). An interference cancellation system for spread spectrum communication channels with cochannel FM interferers, in *Proc. IEEE 39th Midwest symposium on Circuits and Systems*, Ames, IA.

Rilling, G. and Flandrin, P. (2008). One or two frequencies? The empirical mode decomposition answers. **56**: 85–95.

Rilling, G., Flandrin, P. and Gonçalvés, P. (2003). On empirical mode decomposition and its algorithms, in *Proc. IEEE-EURASIP Work. Nonlinear Signal Image Process.* (*NSIP*), Grado, Italy.

Roy, A. and Doherty, J. F. (2008). Empirical mode decomposition frequency resolution improvement using the pre-emphasis and de-emphasis method, in *Proc. 42nd Ann. Conf. Info. Sciences Syst.* (*CISS*), Princeton, NJ.

Roy, A. and Doherty, J. F. (2010). Raised cosine filter-based empirical mode decomposition. *IET Signal Processing*, accepted for publication.

Stevenson, N., Mesbah, M. and Boashash, B. (2005). A sampling limit for the empirical mode decomposition, in *Proc. 8th Int. Symp. Signal Process. Its Appl.* (*ISSPA*), Sydney, Australia, pp. 647–650.

Xuan, B., Xie, Q. and Peng, S. (2007). EMD sifting based on bandwidth. *IEEE Signal Process. Lett.*, **14**: 537–540.

Zhao, L. and Haimovich, A. M. (2002). Performance of ultra-wideband communications in the presence of interference. **20**: 1684–1691.